2024 IEEE International Conference on Robotics and Automation (ICRA 2024)
May 13-17, 2024. Yokohama, Japan

A Miniature 1R1T Precision Manipulator with Remote Center of Motion for Minimally Invasive Surgery

Hiroyuki Suzuki
Sony Computer Science Laboratories, Inc.

***Abstract*— In robotic-assisted minimally invasive surgery, the remote center of motion (RCM) achieves precision and safe manipulation of surgical devices through the insertion point into the patient's body. One of the RCM configurations, one-rotation and one-translation (1R1T) RCM based on a closed-loop design, enables two-degrees-of-freedom transmission from the proximal end of the robotic arm to the distal end. This feature offers important advantages, particularly in enhancing safety by minimizing physical contact risks with patients or other surgical tools owing to the simplified layout near the surgical field. However, conventional 1R1T RCM robots typically employ complex structures with numerous joints consisting of pin-and-hole mating mechanisms. This complexity can increase the overall size of the robot and compromise motion precision. This study presents a miniature 1R1T precision manipulator with RCM, ORIGANOID (dimensions: W60 x D120 x H30 mm, weight: 12.6 g). The robotic arm features flexure hinges, eliminates clearance issues, and can be fabricated using an origami-inspired robotic approach. Furthermore, using a novel backlash-free coupling method, the robotic arm could be easily attached and detached from the drive units. A prototype was fabricated and experimentally validated. The results demonstrated that high-resolution motion could be achieved within 10 µm. Furthermore, a demonstration using an eyeball model confirmed the successful implementation of 1R1T RCM.**

I. Introduction

Significant advancements have been made in minimally invasive surgery (MIS) owing to the growth of teleoperated robotic technology, which provides precise manipulation within a patient's body. Retinal surgery is one of the most complicated forms of MIS, requiring tasks on the µm scale and delicate procedures. Microoperation in the confined space of the eye is challenging because of the pivot motion of the devices via a small insertion point on the fragile sclera under approximately 200 µm hand tremors. Tremor filtering and motion scaling through teleoperation expand the capabilities of a surgeon. Notably, this technology has found its way into clinical applications in retinal surgery [1].

Surgical manipulators for MIS typically require a remote center of motion (RCM) to enable pivotal motion at the insertion point on the patient's body. A common practice is to mechanically constrain the motion of surgical devices to rotate about an RCM (mechanical RCM) because of its safety, ergonomic, and accuracy advantages. Both commercial products and numerous research groups adopted mechanical RCM with various designs [2]. However, the kinematic design often complicates the mechanical structure and increases the size of the robots. These bulky robots carry the potential risk of physical contact with the patient's body and other surgical tools during surgery. In addition, machine vibrations caused by mechanical resonance can degrade the precision of manipulation during delicate tasks. Therefore, downsizing and reducing the weight of these robots have been significant areas of focus.

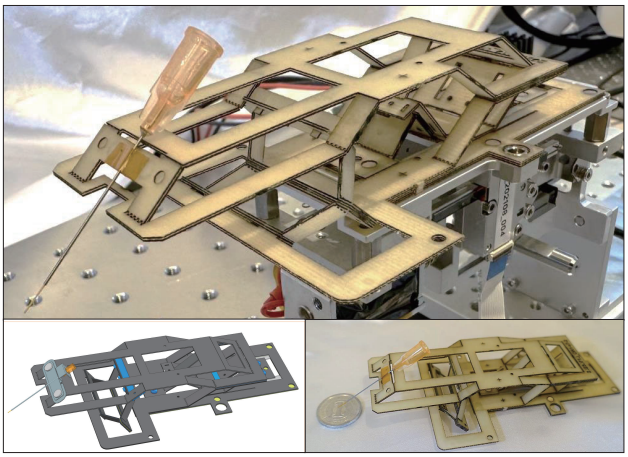

Fig. 1. ORIGANOID: a prototype of the miniature 1R1T RCM robot. The figure in the lower right corner compares the detached robotic arm and a 1 yen coin. The dimensions in terms of volume are W60 x D120 x H30 mm, and it weighs 12.6 g.

We previously introduced an origami-inspired miniature manipulator with a mechanical RCM for MIS [3]. The compact and simplified configuration allows us to leverage the inherent advantages of mechanical RCM and compensate for volumetric disadvantages. This robot had a precision of approximately 20 µm and a compact palm-sized body. However, this preliminary study still had issues related to meeting medical requirements. These issues encompass safety concerns associated with the actuator mounted on the distal end of the robot and the necessity for structural separation between clean and unclean areas.

Conventional surgical manipulators have frequently utilized a kinematic configuration featuring a mechanical RCM linked in series with a translational axis, which moves along the long axis of the surgical tool [4]. This configuration offers advantages in terms of ease of implementation and a relatively large range of motion. However, the translational motion axis at the distal end of the arm can introduce several serious risks, including physical contact with the patient's body or other surgical tools, occlusion of micro-

*This work was not supported by any organization
Hiroyuki Suzuki is with Research Lab., Sony Computer Science Laboratories, Inc., Tokyo, Japan H.Suzuki@sony.com

scopic images, and interference with the sterilization process. To address these issues, researchers have explored the one-rotation and one-translation (1R1T) RCM mechanism, which is characterized by a closed-loop mechanism with two degrees of freedom (DoF) transmission systems. This mechanical configuration allows the integration of two axes into the proximal end of the robotic arm and simplifies the structure of the distal end of the arm near the surgical field [5]. However, 1R1T RCM robotic arms often have complex and large structures owing to their numerous passive joints and linkages.

Another crucial aspect regarding transmission systems for achieving precise manipulation is the configuration of the de-coupling method for the separation of clean and unclean areas. The backlash between the drive and driven shaft couplings worsens the motion precision. Additionally, complex coupling mechanisms with mechanical tools are not ideal because non-engineers typically handle surgical tools and robots in operating rooms. Therefore, innovative coupling approaches are required to ensure precise manipulations in this field.

This study aims to introduce a miniature and precise 1R1T RCM manipulator designed for MIS. Retinal surgery was chosen as a representative example of an MIS application that demands precise and delicate tasks through insertion points. This study presents a novel robotic arm called ORIGANOID, which is manufactured using an approach based on a mechanical structure that combines a rigid frame and flexure hinge. This robot incorporates a novel backlash-free coupling mechanism, enabling the transmission of micromovements from the drive shaft to the end effector with high precision. A validation process was conducted to assess motion precision, and simulations were performed using a model tailored to the target application, utilizing the prototype.

This paper is organized as follows: Section II provides the survey results of the related studies on RCM robots. Section III introduces the design concept and methodology of the proposed robot. Section IV offers a detailed description of the experimental evaluation system. Section V presents the experimental results. Section VI discusses the significance and limitations of the proposed methodology based on experimental results. Finally, Section VII presents conclusions and future work.

II. RELATED WORKS

RCM approaches can be categorized into design- and control-based strategies based on their technical background [6]. The design-based strategy achieves RCM through a kinematic design, often involving parallelograms (mechanical RCM), whereas the control-based strategy is based on a control algorithm for solving the inverse kinematics problem (virtual RCM).

Mechanically constrained RCM offers several advantages, including intrinsic safety, precision, and an intuitive setup for aligning the insertion points on the patient's body with the RCM position. Various precision surgical manipulators have been developed for MIS, such as parallel linkage-based surgical manipulators [7], [8] and arc linear guide-based robots designed for ophthalmic surgery [9]. One of the variations of the mechanical RCM, known as the 1R1T RCM based on pantograph structures, enables the transmission of translational and rotational motions from the proximal end to the distal end of the arm [10]. This feature is preferred in MIS scenarios involving multiple surgical tools near the surgical field. Various types of 1R1T RCM robots were proposed [5], [10], [11], and a common feature of these robots is the presence of numerous passive joints with shaft and hole connections. A complex structure comprising various mechanical components can lead to motion errors owing to passive joint backlash and the problems associated with this complexity.

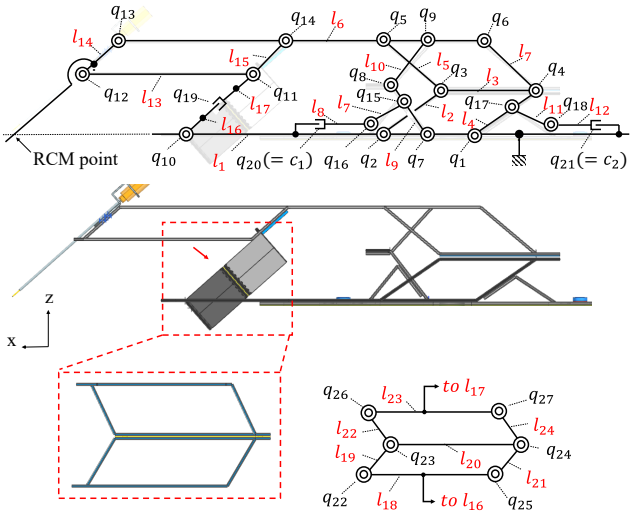

Fig. 2. Schematic overview of ORIGANOID. The robot comprises 24 links and 27 joints. Joints q_{20} and q_{21} can be connected to linear actuators via coupling.

Virtual RCM achieves a pivot motion through a control algorithm with a simple configuration of robotic arms, such as serial linkage robots. Several types of virtual RCM robots exist, including those utilizing linear actuators and gimbal mechanisms [12], employing multiple linear stages [13], and based on serial linkages for handheld interfaces [14]. These methods offer the advantages of a reduced size and simplified robot structure. However, potential safety risks exist owing to calculation errors and unstable motion control when constraining the RCM position at fragile and small insertion points.

III. DESIGN AND FABRICATION

This section delineates the essential specifications of a robot prototype with a specific target application. The design concept and fabrication methods employed based on these specifications are elucidated. Next, the system software encompassing the motion control of the prototype is discussed.

A. Design Goals

The intended application of retinal surgery necessitates specific kinematic constraints involving RCM and micro-

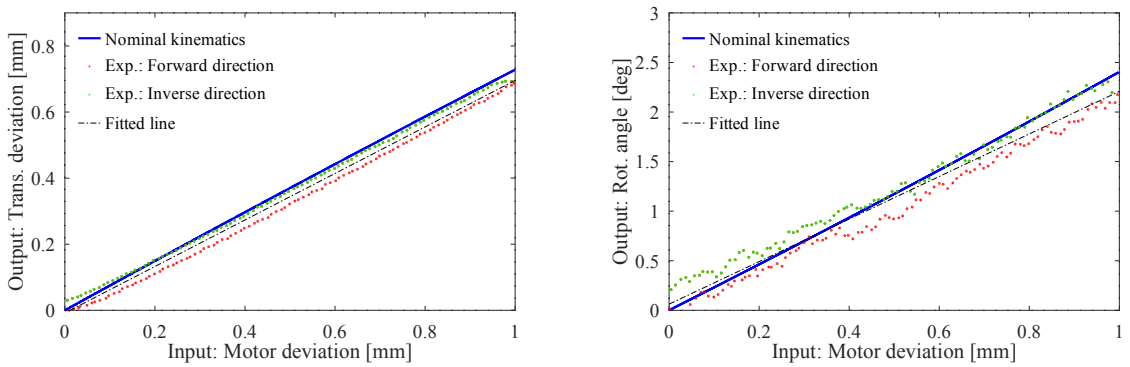

Fig. 3. Kinematic analysis results. The figure includes the evaluation results of hysteresis experiments. Characterizing the relationship between the input deviation and one of the output parameters exhibits high linearity.

manipulation. The target resolution for the end effector's mobility in the direction along the tool is set at 10 µm, corresponding to one-tenth of a thickness of 100 µm for retinal vasculature. The overall range of motion for this prototype is set to approximately 5 mm, and the manipulator will be used with a robot arm with an even greater range of motion to cover an eyeball size. The necessary range of rotational motion was determined to be 15° by calculating the distance from the RCM point to the retina and the required motion range in the horizontal direction, which covers the size of the macula. Table 1 shows the requirements for this study and the specifications of the control system developed.

B. Design and Fabrication of the Origami-based 1R1T Robotic Arm

The robotic design incorporates a pantograph structure consisting of rigid links and flexure hinges, specifically tailored to align with the fabrication technique used for origami-inspired robots. In contrast to our previous research [3], where all passive joints were constituted of flexible rotating hinges, the mechanical configuration in this study incorporates passive slider joints. The slider joints are enabled to have a smooth sliding motion by meticulously adjusting the thickness of the laminated plate material. Figure 1 prominently presents the resulting prototype, while Fig. 2 offers a schematic overview of the designed robotic arm. l_1 through l_{24} represent the links, and q_1 through q_{27} represent the joints. q_{19}, surrounded by l_{16} and l_{17}, which draws a 2 DoF pantograph structure inspired by music stands. This configuration coordinates the direction between l_{16} and l_{17} with that of l_{15}. Additionally, l_{16} is equipped with an end-effector in the form of a needle. The arm has a total of 2 DoF, namely a rotation around the RCM point and a translation along the longitudinal axis. The driven axes, denoted as q_{20} (= c_1) and q_{21} (= c_2), are coupled to the drive axes mounted on the drive units.

The sliding motion of q_{20} and q_{21} is responsible for transmitting translation (trans.) and rotation (rot.) at the distal end, respectively. Figure 3 displays the outcomes of the kinematic analysis of this transmission, performed using software (Siemens Inc., NX). The distance that requires particularly high precision is confined to the range of motion in the direction along the tool near the retina, which is set to 1 mm. Within the motion range, the relationship between input from q_{20} (q_{21}) and output trans. and rot. demonstrates a nearly linear correlation, respectively.

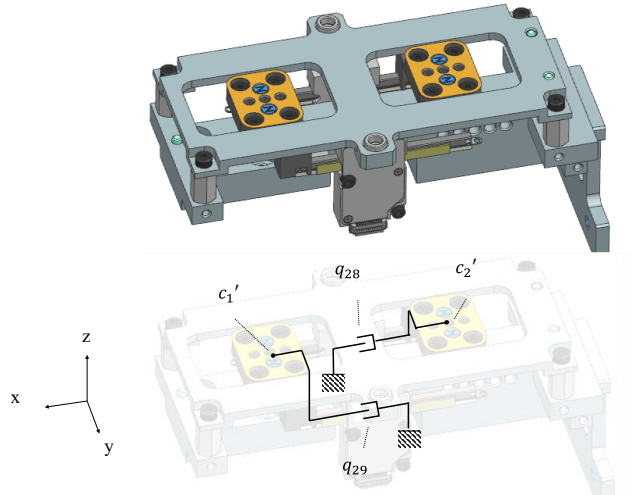

Fig. 4. Schematic overview of the drive unit, which comprises two linear actuators connected to coupler elements c_1' and c_2'.

TABLE I
SPECIFICATIONS OF THE DEVELOPED SYSTEM.

Robot	Degrees of Freedom	2 (1R1T)
	RCM	yes (Mechanical)
	Motion range	∼5 mm, ∼15°
	Resolution	∼10 µm
	Actuation force	∼20 mN [1]
	Actuator	Xeryon inc, XLA-1
	Weight	12.6 g
	Size	W60 x D120 x H30 mm
Microscope	Stereo	Leica, S9D
	Camera	Omron, STC-HD853HDMI
	Digital	ANMO, Dino-Lite edge
System	PC	DELL, Intel Core i7-1255U
	OS	Linux, ubuntu ver.20.04
	ROS	Noetic

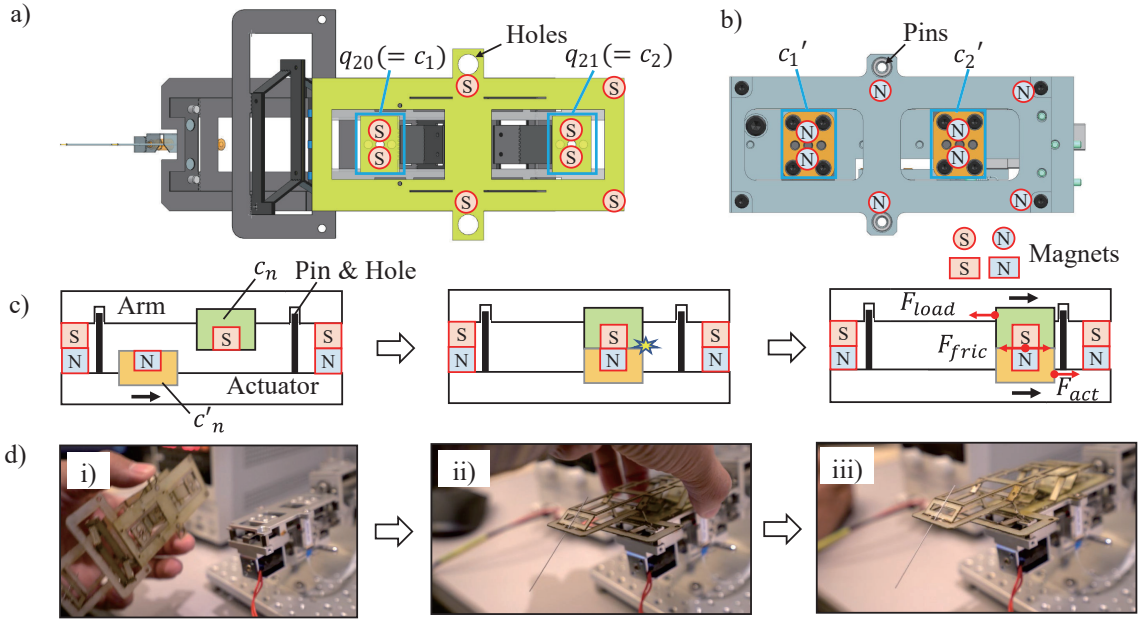

Fig. 5. Mechanical configuration and demonstration of the easy handling of the developed magnetic coupling mechanism. a) and b) ORIGANOID and the drive unit are equipped with permanent magnets, holes, and pins for alignment. c) The coupler elements of the drive unit, denoted as c'_n, and the driven unit, denoted as c_n, can be automatically connected during the origin-detecting motion. d) The process depicts the sequence from coupling to robotic motion (i–iii).

Figure 4 shows the schematic overview of the drive unit. Two linear actuators, q_{28} and q_{29}, allow the motion of c'_1 and c'_2 in the direction of the x-axis. Furthermore, c'_1 and c'_2 can be coupled with c_1 and c_2. Piezo-based linear actuators were used for their unique ability to maintain position during a power outage due to friction. This feature provides inherent safety by avoiding unintended movements owing to weight.

Figure 5 illustrates a backlash-free magnetic coupling method. The drive unit is equipped with permanent magnets on c'_1 and c'_2, oriented in a polarity that allows them to exert an attractive force on the magnets mounted on c_1 and c_2 (Fig. 5-a). Similarly, magnets were affixed to the mechanical bases of the drive and arm units. The magnetic attraction facilitates a straightforward connection between the arm and the drive unit, which is accomplished through a simple attachment process using pin-and-hole mating (Fig. 5-a, b). Furthermore, even if the initial positions of the driven parts c_n and drive parts c'_n are not aligned, the connection can be automatically established at the correct position during the initial motion (Fig. 5-c).

Backlash-free driving of c_n by c'_n without slipping occurs when the following conditions are met:

$$F_{fric} > F_{act} + F_{load}$$
$$F_{act} > F_{load}$$

Here, F_{fric} represents the maximum static friction force between c_n and c'_n, F_{act} is the driving force generated by the actuator, and F_{load} is the reactive force applied to c_n from the end-effector's contact force. Figure 5-d illustrates the workflow from coupling to robotic motion (Supplementary Video).

Notably, this coupling method eliminates the need for complex tasks, such as tightening screws and nuts, which are typically associated with conventional couplers.

To fabricate the prototype, a fabrication process inspired by a previous study [3] was employed, utilizing a combination of laser processing and heat pressing. The rigid link frame was constructed from glass fiber-reinforced plastic (FR4) with a thickness of approximately 0.3 mm, while flexible joints were made from polyester (TORAY, Rumilar) with a thickness of 38 µm. Thermosetting adhesive sheets (Toyochem Co., Ltd., TSU0041SI35 DL) were used to bond these components together. Initially, they were fabricated using a laser cutting machine (Laser Systems Inc., UV, 6W power) and heat-press equipment. Heat-resistant neodymium magnets were used in the coupling mechanism (NEOMAG, N35EH).

Figure 6 illustrates the architecture of the developed system, which is based on the robot operating system (ROS). This system comprises several key subroutines: 1) a node connected to human interface devices (node_joystick, node_footswt), 2) a node responsible for implementing posi-

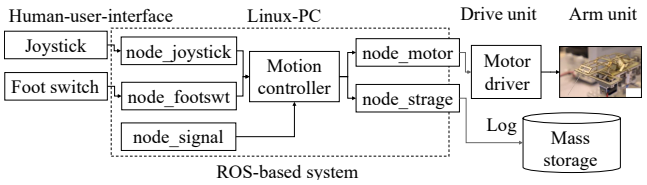

Fig. 6. ROS-based motion control system connected to human-user interface devices and actuators through a motor driver.

tion proportional control (motion controller), 3) a node designed for networking with motor drivers (node_motor), and 4) a node that serves as a signal generator for experimental purposes (node_signal).

IV. EXPERIMENTAL SETUP

In this section, the experimental method for evaluating the characteristics and conducting phantom tests to simulate the target application is introduced.

To assess the micro-scale manipulation without contact, an experimental system utilizing a video microscope was constructed, as depicted in Fig. 7. This setup involved mounting a measurement scale featuring a 100-µm grid pattern onto a three-DoF micro linear stage. A test probe is affixed to the distal end of the prototype. The position of the probe tip was captured using a video microscope (ANMO, Dino-Lite Edge), and the recorded data were subsequently analyzed to extract the time-series translational and rotational displacements.

Figure 8 shows the experimental setup employed to assess the feasibility of this approach, utilizing an eye-model designed to simulate the target application. This experiment aimed to demonstrate pivotal movements around the insertion point and micromanipulation with free motion. The fabricated eye model was affixed to a gimbal featuring two holes at its center for bottom observation and test probe insertion. The eye model was produced using a 3D printer and incorporated micro-landmarks measuring between 0.05 to 0.4 mm at its base. An image of the operational field was captured using a stereomicroscope equipped with a camera (Omron, STC-HD853HDMI). The operator can manipulate the test probe using a joystick or button.

V. EXPERIMENTAL RESULTS

This section presents the experimental results (N=5): 1) the hysteresis characteristics obtained from the ramp input test, 2) the motion response characteristics observed during the 100 µm-step input test, and 3) the motion response characteristics recorded during microscale input test.

The motion response results for translation and rotation were observed when ramping inputs at a velocity of 0.1 mm/s in the forward and reverse directions in order (Fig. 9-left). A comparison between the calculated and evaluated kinematics is shown in Fig. 3. The hysteresis error was evaluated, with the trans. as 0.019 mm, and the rot. as 0.138°. The nonlinear features of flexure hinges can cause hysteresis. The positional and rotational deviation were measured using a step signal to assess the micro-response. Figure 9-center shows the results of the deviation in the translational axis when a 100-µm step was input into q_{20}. The magnitude of each step peak for the previous motion step was evaluated in trans.: 70±4.5 µm.

The micro-response characteristics driven by micro-scale input motion were also assessed. Figure 9-right illustrates the mean translational deviation of the probe tip when a 10-µm command signal was applied. The peak value of each step was measured as 7.5±2.5 µm. These results demonstrate that the prototype exhibited a high motion resolution within 10 µm. The trajectory closely tracks the calculated nominal values; however, a hysteresis error can arise because of the nonlinear characteristics of the compliant characteristic.

The feasibility of scanning the tool within the eyeball was assessed using an experimental system that utilized simulated eyeballs (Fig. 10). The test probe inserted into the eyeball can be manipulated without contacting the ϕ3 insertion hole. The results demonstrated that 1R1T motion was successfully achieved (see Supplementary Video).

VI. DISCUSSION

This study presents an origami-inspired precision miniature 1R1T RCM manipulator with a novel backlash-free coupler between the drive and driven axes. Reducing size and weight is crucial for achieving high motion precision and minimizing potential risks, including physical contact, to enhance the efficiency and safety of operational outcomes in

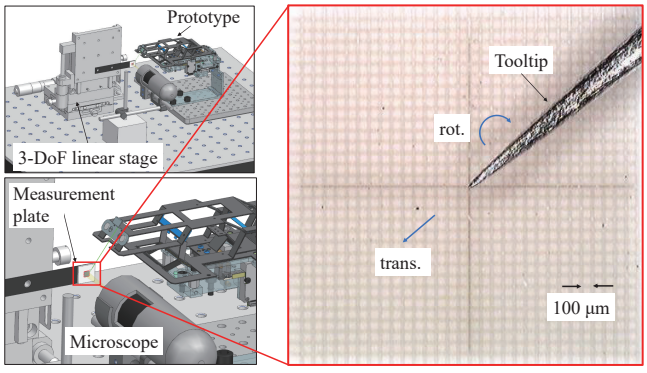

Fig. 7. Experimental setup for validating the characteristics of the fabricated prototype included a measurement scale near the tip of the probe at the distal end of the arm. A video microscope captured the motion of the tip, and the trajectory was analyzed based on the recorded images.

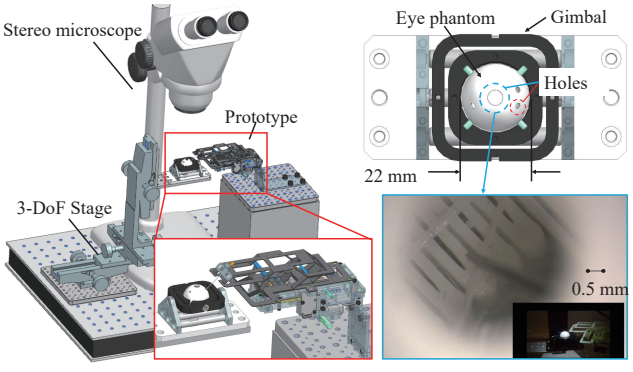

Fig. 8. Demonstration of the 1R1T motion featuring a simulated eyeball phantom is performed. An eyeball model, attached to a gimbal, incorporates apertures for observing the operational field through a stereo microscope and inserting the testing tool.

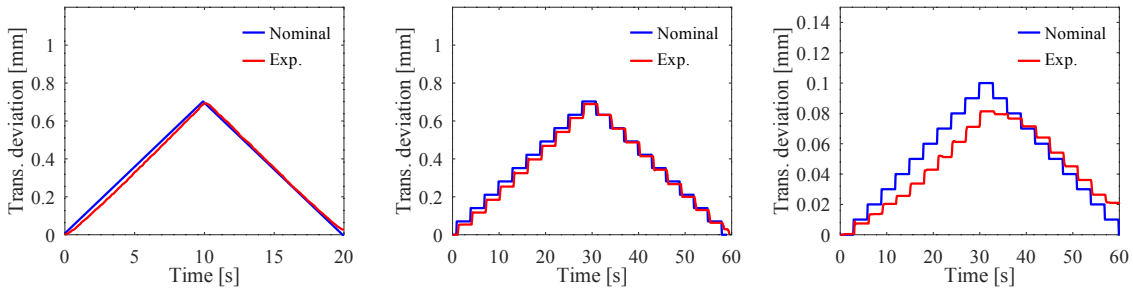

Fig. 9. Characteristic evaluation results. The output of translational deviation resulting from left) ramp input, center) 100μm stairs input, right) 10μm stairs command at the tooltip.

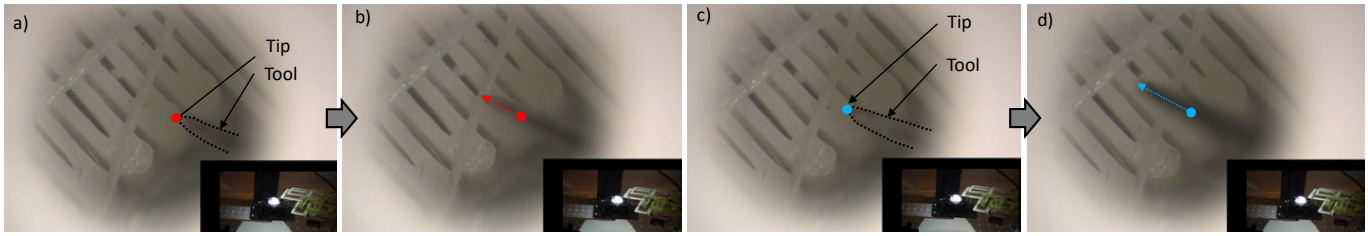

Fig. 10. Trajectories of translational (a–b) and rotary (c–d) tool motion with an RCM point. Marked-up red and blue circles indicate the initial position of the tooltip during translational and rotary motion, respectively.

robotic-assisted MIS. Integrating all actuators at the proximal end of the arm using 1R1T RCM mechanisms allows for a simple structure at the distal end near the surgical field. The prototype of a 1R1T manipulator (W60 x D120 x H30 mm, 12.6 g) was fabricated using an origami-inspired robotic approach. The results of the characteristic evaluations of the motion resolution showed a resolution of 7 μm, a marked improvement from the approximate 20 μm resolution observed in our prior research. Furthermore, a simulated eyeball demonstration shows the pivot motion around the tool's insertion point and micro-free motion commanded through a human-user interface.

The robot is equipped with a backlash-free magnetic coupler. This novel coupled system has the advantages of high motion resolution and minimal loss of motion. Furthermore, a simplified structure without screw nuts is preferable to allow non-engineers to assemble it in the operating room.

The motion system is developed based on a ROS and is expected to be extended to navigation using sensing information from OCT and automatic control using machine learning to recognize lesions as objects. Researchers have reported navigation for cataract surgery using OCT images, and automatic puncture of the fundus blood vessels has been performed [9], [15]. For motion control, we demonstrated the functioning of a 1R1T RCM through kinematic analysis employing CAD-based simulation software, complemented by experimental verification via an eye phantom test. In the future, the analytical or numerical solutions of kinematics serve to facilitate the optimization of the 1R1T design, including an analysis of operability subject to the constrained workspace.

In this study, several technical aspects must be further developed for clinical application. First, this study focused on achieving a miniature configuration of 1R1T with two DoF, whereas a total of three DoF is typically required for MIS. Therefore, future work is needed to incorporate an additional rotational axis into the robot design, as researchers have introduced 1R1T RCM robots connected to a rotation axis in series [16]. Second, a hysteresis error was observed during the experimental motion (approximately 20 μm). The proposed robot relies on a mechanical structure that combines a rigid frame and flexure hinge, which can lead to nonlinear characteristics. Optimization of the hinge material or geometric features is necessary to enhance precision. Third, the experimental tests were limited to dry model tests, and specific challenges arose when working with living organisms. For instance, frictional forces between the trocar and surgical tools are encountered in an actual operation. To address these issues, feasibility tests in vivo are necessary in future research.

VII. CONCLUSION

This study introduced an ultra-compact and highly precise origami-inspired 1R1T RCM manipulator. Moving forward, the study will address these limitations and encompass medical engineering investigations, including in-vivo trials.

ACKNOWLEDGMENT

The author would like to acknowledge the advice regarding the clinical application of Dr. Masayo Takahashi, Dr. Tadao Maeda, and all persons involved in this research.

REFERENCES

[1] E. Vander Poorten, C. N. Riviere, J. J. Abbott, C. Bergeles, M. A. Nasseri, J. U. Kang, R. Sznitman, K. Faridpooya, and I. Iordachita, "36 - robotic retinal surgery," in *Handbook of Robotic and Image-Guided Surgery.*, M. H. B. T. H. o. R. Abedin-Nasab and I.-G. Surgery, Eds. Elsevier, 2020, pp. 627–672.

[2] R. H. Taylor, A. Menciassi, G. Fichtinger, P. Fiorini, and P. Dario, *Medical Robotics and Computer-Integrated Surgery BT - Springer Handbook of Robotics*. Cham: Springer International Publishing, 2016, pp. 1657–1684.

[3] H. Suzuki and R. J. Wood, "Origami-inspired miniature manipulator for teleoperated microsurgery," *Nat. Mach. Intell.*, 2020.

[4] S. Aksungur, "Remote center of motion (RCM) mechanisms for surgical operations," *Int. J. Appl. Math. Elec. Comput.*, vol. 3, p. 119, Mar. 2015.

[5] H. Long, Y. Yang, X. Jingjing, and S. Peng, "Type synthesis of 1R1T remote center of motion mechanisms based on pantograph mechanisms," *J. Mech. Des.*, vol. 138, no. 1, Jan. 2016.

[6] Z. Wang, W. Zhang, and X. Ding, "A family of RCM mechanisms: Type synthesis and kinematics analysis," *Int. J. Mech. Sci.*, vol. 231, p. 107590, Oct. 2022.

[7] T. L. Edwards, K. Xue, H. C. M. Meenink, M. J. Beelen, G. J. L. Naus, M. P. Simunovic, M. Latasiewicz, A. D. Farmery, M. D. de Smet, and R. E. MacLaren, "First-in-human study of the safety and viability of intraocular robotic surgery," *Nat. Biomed. Eng.*, vol. 2, no. 9, pp. 649–656, 2018.

[8] A. Gijbels, J. Smits, L. Schoevaerdts, K. Willekens, E. B. Vander Poorten, P. Stalmans, and D. Reynaerts, "In-Human Robot-Assisted retinal vein cannulation, a world first," *Ann. Biomed. Eng.*, vol. 46, no. 10, pp. 1676–1685, 2018.

[9] C.-W. Chen, Y.-H. Lee, M. J. Gerber, H. Cheng, Y.-C. Yang, A. Govetto, A. A. Francone, S. Soatto, W. S. Grundfest, J.-P. Hubschman, and T.-C. Tsao, "Intraocular robotic interventional surgical system (IRISS): Semi-automated OCT-guided cataract removal," *Int. J. Med. Robot.*, vol. 14, no. 6, p. e1949, Dec. 2018.

[10] J. Smits, D. Reynaerts, and E. V. Poorten, "Synthesis and methodology for optimal design of a parallel remote center of motion mechanism: Application to robotic eye surgery," *Mech. Mach. Theory.*, vol. 151, p. 103896, Sep. 2020.

[11] W. Ye, B. Zhang, and Q. Li, "Design of a 1R1T planar mechanism with remote center of motion," *Mech. Mach. Theory.*, vol. 149, p. 103845, Jul. 2020.

[12] M. Nambi, P. S. Bernstein, and J. J. Abbott, "A compact telemanipulated Retinal-Surgery system that uses commercially available instruments with a Quick-Change adapter," *J. Med. Robot. Res.*, vol. 01, no. 02, p. 1630001, Jun. 2016.

[13] M. A. Nasseri, M. Eder, D. Eberts, S. Nair, M. Maier, D. Zapp, C. P. Lohmann, and A. Knoll, "Kinematics and dynamics analysis of a hybrid parallel-serial micromanipulator designed for biomedical applications," in *2013 IEEE/ASME International Conference on Advanced Intelligent Mechatronics*, 2013, pp. 293–299.

[14] B. Mitchell, J. Koo, I. Iordachita, P. Kazanzides, A. Kapoor, J. Handa, G. Hager, and R. Taylor, "Development and application of a new Steady-Hand manipulator for retinal surgery," in *Proceedings 2007 IEEE International Conference on Robotics and Automation*. ieeexplore.ieee.org, Apr. 2007, pp. 623–629.

[15] M. D. de Smet, T. C. M. Meenink, T. Janssens, V. Vanheukelom, G. J. L. Naus, M. J. Beelen, C. Meers, B. Jonckx, and J.-M. Stassen, "Robotic assisted cannulation of occluded retinal veins," *PLoS One*, vol. 11, no. 9, p. e0162037, Sep. 2016.

[16] A. Gijbels, E. B. V. Poorten, P. Stalmans, H. Van Brussel, and D. Reynaerts, "Design of a teleoperated robotic system for retinal surgery," in *2014 IEEE International Conference on Robotics and Automation (ICRA)*, 2014, pp. 2357–2363.